

Micellization of Sodium Decyl Naphthalene Sulfonate Studied by ^1H NMR

H. Z. Yuan,[†] X. L. Tan,[‡] G. Z. Cheng,[§] S. Zhao,[‡] L. Zhang,[‡] S. Z. Mao,[†] J. Y. An,[‡]
J. Y. Yu,[‡] and Y. R. Du^{*,†}

State Key Laboratory of Magnetic Resonance and Atomic and Molecular Physics, Wuhan Institute of Physics and Mathematics, The Chinese Academy of Sciences, Wuhan 430071, China, Technical Institute of Physics and Chemistry, The Chinese Academy of Sciences, Beijing 100101, China, and
Department of Chemistry, Wuhan University, Wuhan 430072, China

Received: October 7, 2002; In Final Form: February 15, 2003

^1H chemical shift changes of a newly synthesized anionic surfactant, sodium decyl naphthalene sulfonate (SDNS), show that its critical micellar concentration (cmc) lies between 0.82 and 0.92 mM, which is in agreement with that measured by the surface tension method (0.8 mM). The difference in aromatic ring current effect on the naphthyl protons, the different changes in their spin–spin relaxation times upon micellization, and the appearance of cross-peaks between intermolecular protons in the aqueous micellar solution give information about the relative arrangement of the naphthyl rings in the SDNS micelles.

Introduction

Surfactants form orientated colloidal aggregates, micelles, which have been proven to be very useful in many biological and industrial processes. Properties of these systems have been intensively investigated by many spectroscopic methods, especially nuclear magnetic resonance (NMR). It has played a more and more important role with the continued development of NMR new techniques. Characterization of micellization processes, physical properties of micelles, such as structure, size, and shape, hydration, solubilization, and interaction between micelles of different types of surfactants and those with biological compounds and polymers have been studied by the existing sophisticated NMR techniques. These investigations demonstrate that NMR spectroscopy is a versatile technique for the study of micelles.¹ It provides information at a molecular level that is not available by other spectroscopic methods. Chemical shift changes, relaxation experiments, and NMR self-diffusion coefficient measurements have been used almost routinely.^{2,3} The use of the two-dimensional NMR spectroscopy techniques, nuclear Overhauser enhancement spectroscopy (NOESY)^{4–12} and heteronuclear Overhauser enhancement spectroscopy (HOESY),^{13–18} is a growing trend in studying the chain packing in micelles, as well as interactions between micelles with other molecules, including biological molecules and polymers. These methods provide a deeper insight into the relative arrangement of molecules in an associated assembly. Among the anionic sodium sulfonate surfactants, alkyl and alkyl benzene sulfonates received more attention in studying their micellization processes. But the micellization of sodium alkyl naphthalene sulfonate remains less understood. In this article, the packing of the hydrophobic part, especially the naphthyl rings, of the sodium decyl naphthalene sulfonate surfactant in the micellar core will be elucidated by the changes in NMR

chemical shift and spin–spin relaxation of the protons included in the surface layer of the hydrophobic micellar core and by the spatial distances between the protons of interest measured by the 2D NOESY experiments.

Experimental Section

Sodium decyl naphthalene sulfonate (SDNS) was synthesized by the reaction between bromonaphthalene and bromodecane in the presence of metallic sodium and sulfonation by chlorosulfonic acid. The details of the synthesis will be published elsewhere.

D₂O of 99.6% deuterated is the product of Beijing Chemical Factory of China. It was used as received without any purification.

All of the ^1H NMR measurements were performed on a UNITY INOVA-600 with a ^1H frequency of 599.93 MHz. A Carr–Purcell–Meiboom–Gill (CPMG) pulse sequence was used for spin–spin relaxation time (T_2) measurements at 25 °C. D₂O was used as solvent instead of water to weaken the water signal. Meanwhile, a presaturation method was used to further suppress the proton signal of the solvent. 2D NOESY experiments were performed with the standard three-pulse sequence.¹⁹ Mixing times of 1.0 s, 200 ms, and 100 ms were chosen for the system at a concentration of 3.5 mM of sodium decyl naphthalene sulfonate to select a suitable mixing time for the calculation of interproton distances for which spin diffusion effect does not exist so that the evaluated values are reliable. Thirty-two accumulations were collected generally, and 256 accumulations were collected for the dilute solutions of 0.34, 0.52, and 0.7 mM SDNS.

Results

The ^1H NMR spectrum of the synthesized sodium decyl naphthalene sulfonate (SDNS) at a concentration of 0.34 mM in D₂O is shown in Figure 1A. The spectrum is assigned by simulation according to the protons of SDNS labeled in Figure 2. The aromatic proton resonance peaks on the spectrum of the solution at a concentration of 3.51 mM (Figure 1B) are assigned according to the appearance of cross-peaks between protons

* To whom correspondence should be addressed. E-mail: lfshen@wipm.ac.cn.

[†] Wuhan Institute of Physics and Mathematics, The Chinese Academy of Sciences.

[‡] Technical Institute of Physics and Chemistry, The Chinese Academy of Sciences.

[§] Wuhan University.

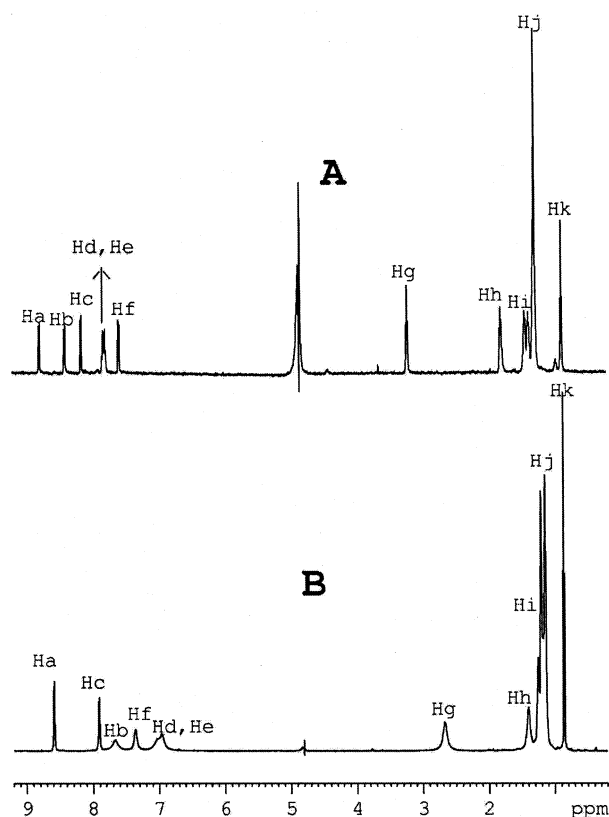


Figure 1. ^1H spectra of sodium decyl naphthalene sulfonate in D_2O solutions at concentrations (A) 0.34 and (B) 3.51 mM.

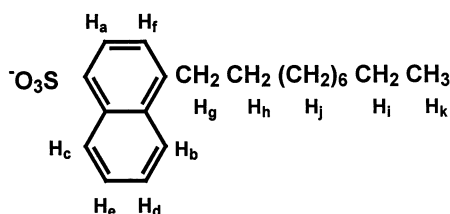


Figure 2. Structural formula and proton labelings of sodium decyl naphthalene sulfonate.

TABLE 1: The Variation in ^1H Chemical Shifts (ppm) of Sodium *p*-n-Decyl Naphthalene Sulfonate with Concentration (mmol/L) in Aqueous Solutions

	[SDNS]								
	0.34	0.52	0.70	0.82	0.92	1.68	2.59	3.51	4.16
H_a	8.69	8.69	8.69	8.69	8.61	8.60	8.60	8.59	8.59
H_b	8.32	8.32	8.32	8.32		7.70		7.67	7.66
H_c	8.07	8.07	8.07	8.07	7.94	7.92	7.93	7.91	7.91
H_d	7.74	7.74	7.73	7.74	7.09	7.07	7.08	7.02	7.01
H_e	7.72	7.72	7.71	7.72	7.03	7.01	7.02	6.96	6.95
H_f	7.51	7.51	7.50	7.51	7.40	7.38	7.40	7.36	7.35
H_g	3.18	3.18	3.18	3.18	2.73	2.70	2.71	2.67	2.66
H_h	1.77	1.77	1.77	1.77	1.45	1.42	1.44	1.40	1.39
H_i	1.41	1.41	1.41	1.41	1.25	1.26	1.24	1.30	1.25
H_j	1.34	1.34	1.34	1.36	1.20	1.20	1.18	1.17	1.16
H_k	0.87	0.87	0.87	0.87	0.85	0.85	0.85	0.85	0.85

attached to adjacent carbon atoms of the naphthyl ring (H_a – H_f , H_b – H_d , and H_c – H_e) on the 2D NOESY map, shown in Figure 3. ^1H chemical shifts of SDNS in aqueous solutions at concentrations of 0.34, 0.52, 0.7, 0.82, 0.92, 1.68, 2.59, 3.51, and 4.16 mM are listed in Table 1. The chemical shifts of all of the protons keep constant between concentrations ranging from 0.34 to 0.82 mM but dramatically shift to lower frequencies with different extent between concentrations of 0.82 and 0.92

mM and then change more gradually as the concentration increases (Figure 4). This shows that the cmc of SDNS lies in this range of concentration, which is in agreement with the cmc (0.80 mM) obtained by the surface tension method. It is worth noticing that the chemical shifts of the aromatic protons (H_a , H_b , H_c , H_d , H_e , and H_f) and those attached to the carbon atoms near the naphthyl ring (H_g and H_h) show larger changes than those on the alkyl chains farther from the naphthyl ring when the concentration increases from 0.82 to 0.92 mM. Meanwhile, the resonance peaks of H_b , H_d , and H_e are significantly broadened as shown in Figure 1A,B. The broadened resonance peaks of H_d and H_e overlapped, and H_d became a shoulder on the peak of H_e . They shifted so much that they lie on the lower-frequency side of the resonance peak of H_f . The same is the case in the changes in chemical shift of H_b . The resonance peak of H_b is broadened and shifted to lower frequency remarkably than that of H_c .

Spin–spin relaxation times (T_2) of the solutions are listed in Table 2. The T_2 values of H_b , H_d , H_e , H_f , and H_g change from 181, 108, 108, 150, and 92 ms at a concentration of 0.34 mM, respectively, to about 10 ms at concentrations above 0.92 mM. This indicates that the motion of these protons becomes seriously restricted at concentrations above 0.92 mM, and they probably participate in the formation of the surface layer of the hydrophobic micellar core.²⁰ Panels A and B of Figure 5 are pictorial representations showing that H_f , H_b , H_d , H_e , and H_g are involved in the surface layer of the micellar core. They have very short spin–spin relaxation times owing to the self-association and have larger changes in chemical shifts owing to the intermolecular aromatic ring current effect.

To examine the evolution of cross-peaks in the 2D NOESY experiment of the 3.51 mM solution, different mixing times of 100 ms, 200 ms, and 1 s have been chosen. Figure 3A–C shows that the cross-peaks are evolving with mixing times. The intensities (relative to each of the intensities of the diagonal peak of H_a for different τ_m 's as 100) of the cross-peaks between H_b and H_f and between H_d and H_f for τ_m of 100 ms, 200 ms, and 1 s are 1.26, 2.65, and 6.28 and 1.09, 3.84, and 6.75, respectively. It is reasonable to choose the lowest mixing time to estimate the distances. Figure 3A is expanded to show clearly the cross-peaks between the aromatic protons (Figure 6). Besides the cross-peaks of the protons attached on adjacent carbon atoms of the naphthyl ring (H_a – H_f , H_b – H_d , H_c – H_e), there appeared cross-peaks between H_d and H_f and between H_b and H_f in the aromatic region. According to the calculation by HYPERCHEM after geometric optimization for a single SDNS molecule (Table 3), the intramolecular spatial distances between these protons should be 4.84 and 6.78 Å, respectively. Protons with such spatial distances would hardly show interactions through space on the 2D NOESY map.

Interproton distances of the protons in the 3.51 mM SDNS solution were calculated from the integrals of the cross-peaks of the 2D map with a mixing time of 100 ms according to the following expression:

$$r_{nm} = r_{ab} \times \sqrt[6]{\frac{I_{ab}}{I_{nm}}}$$

where r_{ab} and I_{ab} are the spatial distance and the intensity of the cross-peak between a pair of protons of known spatial distance and r_{nm} and I_{nm} are those of the cross-peaks between the protons of interest, respectively. In calculation, the interproton distance between H_a and H_f , 2.40 Å, calculated by HYPERCHEM for a single molecule was taken as the known

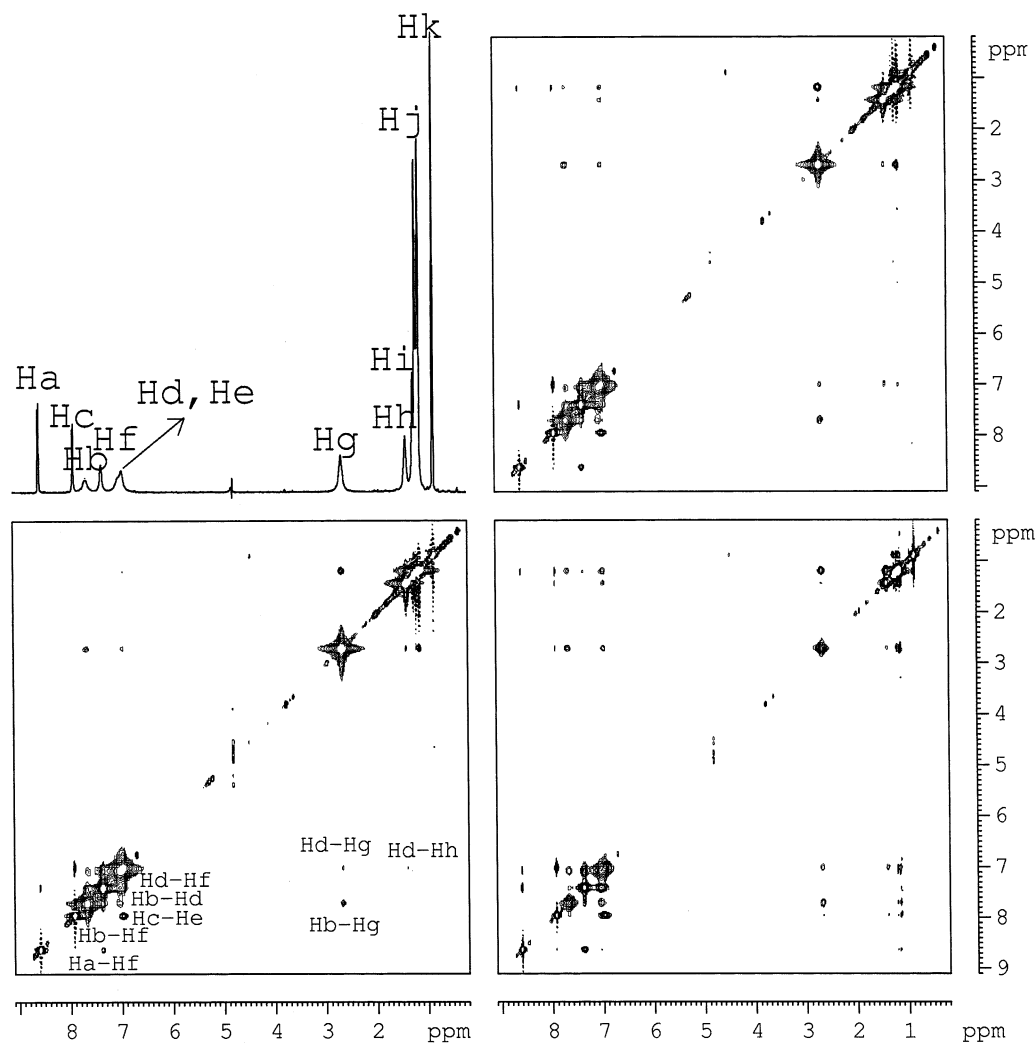


Figure 3. Contour plots of the 2D NOESY map of sodium decyl naphthalene sulfonate solution at a concentration of 3.51 mM with mixing times of (A) 100 ms, (B) 200 ms, and (C) 1 s.

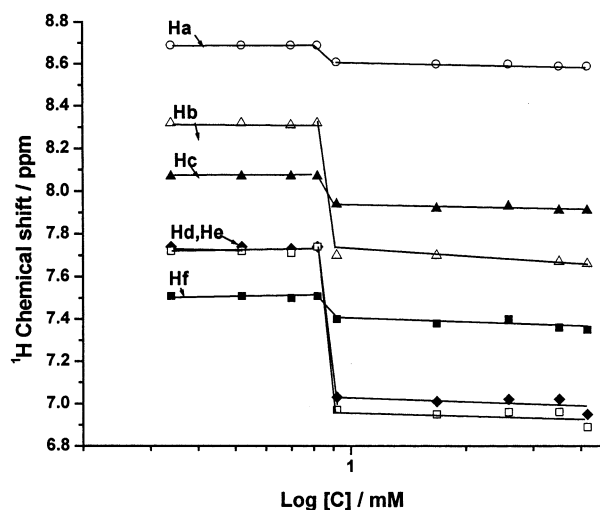


Figure 4. The changes in ^1H chemical shifts of sodium decyl naphthalene sulfonate solution with its concentration.

interproton distance. Several interproton distances calculated from the 2D NOESY map and by HYPERCHEM are listed in Table 3. Comparing these interproton distances in the micellar state with those calculated by HYPERCHEM in which SDNS was assumed to be in the monomer state, one finds that the

TABLE 2: The Variation in T_2 (ms) of Sodium Decyl Naphthalene Sulfonate Protons with Concentration (mmol/L) in Aqueous Solutions

	[SDNS]/cmc					
	0.34	0.92	1.68	2.59	3.51	4.16
H _a	110	50	49	45	49	43
H _b	181		10		10	12
H _c	121	29	48	30	49	57
H _d	108		19		12	13
H _e	108		19		12	13
H _f	150	5	12	8	10	10
H _g	92	12	8	10	8	9
H _h	119	33	30	28	29	30
H _i	192	177	195	163	201	196
H _j	298	70	66	70	89	94
H _k	511	236	227	275	242	301

interproton distances of the protons attached to adjacent carbon atoms, $\text{H}_b\text{--H}_d$ and $\text{H}_c\text{--H}_e$, remain almost unchanged upon micellization within 10% errors. However, the interproton distances between $\text{H}_b\text{--H}_f$ and $\text{H}_d\text{--H}_f$ are shortened from 4.84 to 2.4 Å and from 6.78 to 2.0 Å, respectively, in forming micelles. The interproton distances between $\text{H}_d\text{--H}_g$ and $\text{H}_d\text{--H}_h$ are also shortened from 4.65 to 3.5 Å and from 6.95 to 3.7 Å, respectively. It should be emphasized that in calculating the interproton distances between $\text{H}_d\text{--H}_g$ and $\text{H}_d\text{--H}_h$ it has been

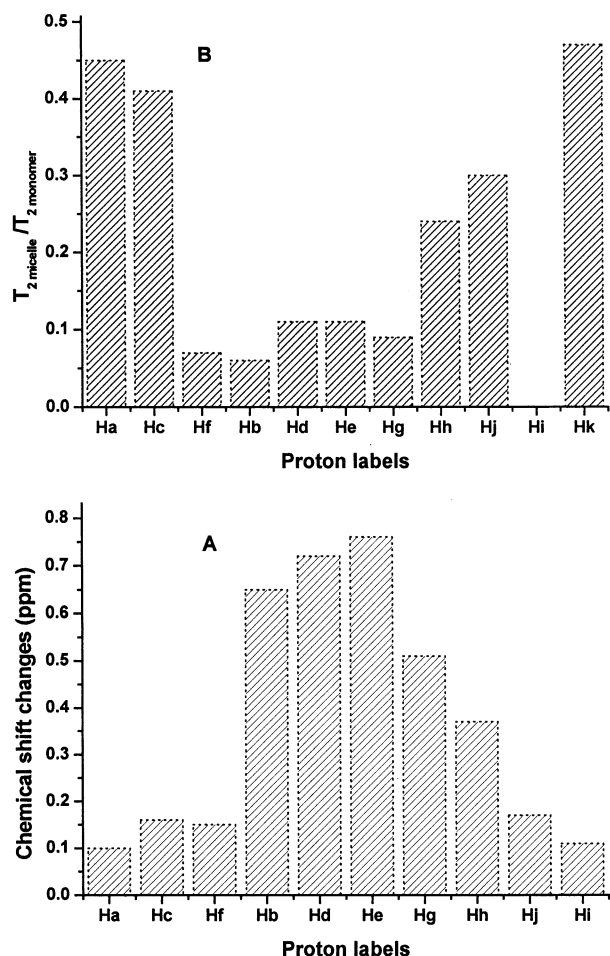


Figure 5. Micellization induced changes in (A) ^1H chemical shifts and (B) spin-spin relaxation times of different protons of sodium decyl naphthalene sulfonate.

considered that there are two H_g protons and two H_h protons interacting with H_d proton, so the integrals of the cross-peaks between $\text{H}_d\text{--H}_g$ and between $\text{H}_d\text{--H}_h$ were divided by two, respectively, in the calculation using the above expression.

Discussion

Critical Micellar Concentration of Sodium Decyl Naphthalene Sulfonate. Figure 4 shows that the chemical shifts of all of the protons remain unchanged at concentrations ranging from 0.34 to 0.82 mM. It shows that there is no change in chemical environment of the SDNS protons in this range of concentrations, so the SDNS molecules are moving freely in the single molecular state. The dramatic decrease in chemical shift within a narrow range of concentration from 0.82 to 0.92 mM shows that a change in the chemical environment of the protons occurs, that is, the single molecules associate at this concentration range (i.e., the cmc). The more gradual decrease in chemical shift on further increase in concentration beyond 0.92 mM is the result of the weighted average of the chemical shifts of the monomers and those of the micelles. It is obvious that the cmc of SDNS is lower than those of the alkyl and alkyl benzene sulfonates, which are 9.7²¹ and 1.2 mM,²² respectively. The reason for this lowering in cmc originates from the difference in chemical structures of the surfactants. The area on the surface layer of the hydrophobic micellar core per polar head of SDNS is larger than those of dodecyl benzene sulfonate and dodecyl sulfonate because the cross sections of the polar

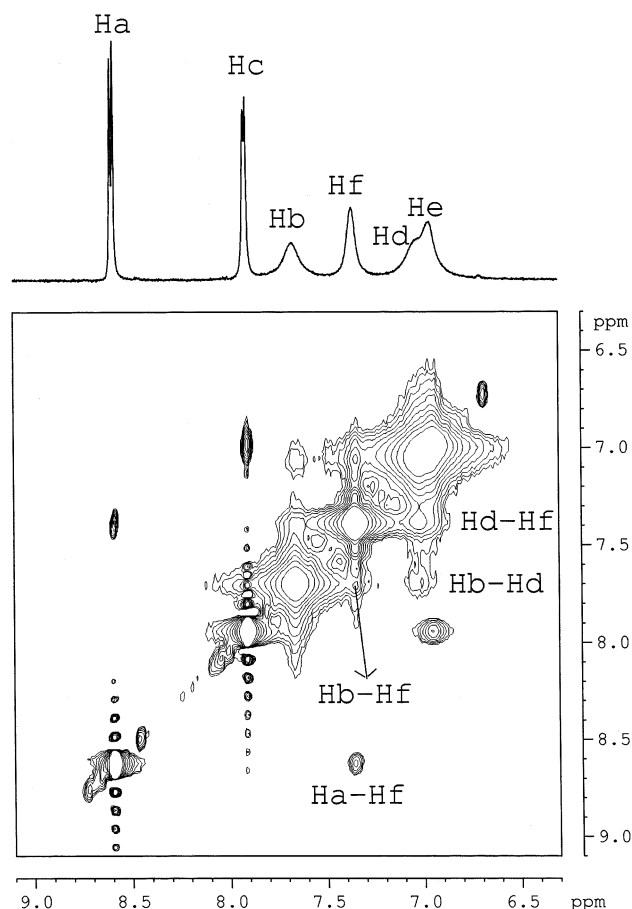


Figure 6. An expansion of the aromatic region from Figure 3A.

TABLE 3: Interproton Distances (\AA) in SDNS Micelles

proton pairs	r_{HYP}	$r_{2\text{D-NOESY}}$
$\text{H}_a\text{--H}_f$	2.40	2.4
$\text{H}_b\text{--H}_d$	2.44	2.6
$\text{H}_b\text{--H}_f$	4.84	2.4
$\text{H}_c\text{--H}_e$	2.43	2.2
$\text{H}_d\text{--H}_f$	6.78	2.0
$\text{H}_d\text{--H}_g$	4.65	3.5
$\text{H}_d\text{--H}_h$	6.95	3.7

heads in these three groups are in the following order: naphthyl ring > benzyl ring > methylene group. So, in forming micelles, the repulsion between the negatively charged sulfonate ions of SDNS is weakened by the increased distance between the polar heads on the surface layer of the hydrophobic micellar core. Consequently, micelles are more easily formed, and a lower cmc for SDNS results.

Arrangement of the Hydrophobic Chains of the Surfactant in the Micellar Core and Their Dynamics. The microstructure and chain dynamics of surfactant micelles have been studied extensively. Spin-lattice relaxation of hydrocarbon chain protons in an aqueous solution of sodium alkyl sulfate indicates that when micelles are formed, the motion of the CH_2 protons is remarkably restricted.²³ Multinuclear chemical shift changes are often used in elucidating structures of micelles^{24–27} among which ^1H chemical shift changes induced by aromatic ring current²⁷ are most effective. It appears either in self-aggregation of surfactants containing aromatic groups or in solubilization of aromatic compounds in ordinary micelles. It has been shown that the ortho and meta protons on the phenoxy ring of Triton X-100 shift to lower frequency upon micellization

because the phenoxy rings get close together in the micelles.²⁸ The aromatic protons of a molecule experience the aromatic ring current effect from other nearby molecules. However, the effect of aromatic ring current on each proton of an aromatic ring in micellization may not be the same. The meta protons of linear alkyl benzene sulfonate shift to lower frequency of 0.25 ppm, while the ortho protons remain unchanged upon micellization. In the case of micellization of sodium decyl naphthalene sulfonate, the naphthyl rings get together resulting in the aromatic ring current effect on the intermolecular protons either on the naphthyl rings or on the alkyl chains. The nearer the proton on the alkyl chain to the aromatic ring, the more obvious is the aromatic ring current effect. The protons on the naphthyl ring also show different changes in chemical shift. Figure 5A shows that the protons on the naphthyl rings, H_b, H_d, H_e, have the largest changes in chemical shift. It suggests that these protons are mostly embedded in the aromatic ring environment. Moreover, the alkyl protons, H_g and H_h, are even more largely affected by the aromatic ring current than the aromatic protons on the naphthyl ring nearest to the sulfonate group, H_a and H_c. Accordingly, the methylene groups on which H_g and H_h are attached seem to be included between the naphthyl rings, whereas the opposite side of the naphthyl ring where the sulfonate group is attached is open. Therefore, on micellization the hydrophobic alkyl chains of the surfactant molecules associate together with the α and β methylene groups embedded between the naphthyl rings, which are packed radiating outward. The difference in behavior of the meta and ortho protons in micellization of linear alkyl benzene sulfonate has been interpreted as different environments experienced by these two protons. The ortho protons exist in the polar environment, while the meta protons are in a hydrocarbon environment.²⁹ It seems that this difference should originate from the difference in the effect of the aromatic ring current. In micellization, the molecules are associated together with the alkyl chains aligned in the interior of the micellar core and the benzyl rings radiating outward to the aqueous medium, so the meta protons are closer to the benzyl rings of other molecules than the ortho protons are, so they experience greater effect from the aromatic ring current and shift to lower frequency.

It has been shown for three types of surfactants (anionic, cationic, and nonionic) that the motion of protons situated on the surface of the hydrophobic micellar core is seriously restricted. The spin–spin relaxation times, T_2 , of these protons are as short as about 10 ms.^{20,28} The spin–spin relaxation times of several protons, (H_d, H_e, H_b, H_f, and H_g) of sodium decyl naphthalene sulfonate at concentrations higher than 0.92 mM (Table 2) are on the order of 10 ms, which are significantly shorter than those of H_a, H_c, and other alkyl protons as shown in Figure 5B and Table 2. So, H_b, H_d, H_e, H_f, and H_g protons probably participate in the formation of the surface layer of the hydrophobic micellar core. This result is in good agreement with that obtained from chemical shift changes. Furthermore, it is worth noticing that from both the chemical shift changes and the spin–spin relaxation data H_h has some opportunity to participate in the formation of the surface layer of the hydrophobic micellar core, because although not so remarkable there are moderate changes in chemical shift; its T_2 value (\sim 30 ms) is shorter than those of the methylene protons farther from the naphthyl ring ($>$ 150 ms). The T_2 decay curve of this proton (Figure 7) shows biexponential behavior. A portion (77%) of this proton has a T_2 value of 17 ms, and the rest has a value of 98 ms. It suggests that the main part of this proton participates in the formation of the surface layer of the hydrophobic micellar

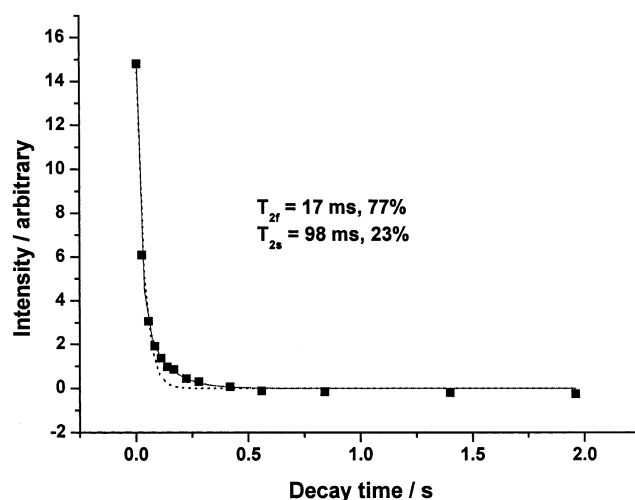


Figure 7. Biexponential behavior of the spin–spin relaxation decay curve. Solid line represents the biexponential fit, and the dotted line represents the ordinary exponential fit.

core, while a small part remains in the interior of the micellar core moving more freely.

The relative arrangement of the surfactant molecular chains in the micelles can be clearly shown by the 2D NOESY experiment.^{4–6} It is clear from Figure 6 that in the aromatic region besides the three cross-peaks of intramolecular interactions between H_a and H_f, H_b and H_d, and H_c and H_e there appeared cross-peaks from intermolecular interactions between H_b and H_f, H_d and H_f, H_d and H_g, and H_d and H_h. The reason for assigning the cross-peaks between H_a and H_f, H_b and H_d, and H_c and H_e as the result from intramolecular proton interactions is that their interproton distances in the micellar state calculated from the intensity of cross-peaks, $r_{2D-NOESY}$, are almost identical with those calculated by HYPERCHEM on the basis of a single molecule as shown in Table 3. However, in the micellar state the interproton distances, $r_{2D-NOESY}$, between H_f and H_b and between H_f and H_d are significantly shorter than those in the single molecular state, r_{HYP} . Because the naphthyl ring is rigid, there is no reason for this remarkable decrease in intramolecular interproton distances between these proton pairs, from 4.84 to 2.4 and from 6.87 to 2.0 Å for H_b–H_f and H_d–H_f, respectively. Therefore, this decrease in interproton distance should originate from intermolecular interaction in the micelles, that is, some special arrangement of the naphthyl rings on the surface layer of the hydrophobic micellar core. The unique probability is that to weaken the repulsion between the negatively charged sulfonate polar groups upon micellization the unsubstituted halves of the naphthyl rings are embedded between the halves substituted by the sulfonate groups of other sodium decyl naphthalene sulfonate molecules. This results in the shortening of the interproton distances between H_f and H_b and between H_f and H_d. The problem is that according to this arrangement of the naphthyl rings the interproton distances between H_a and H_c and between H_a and H_e should also show shortenings from the single molecular state (6.79 and 4.87 Å, respectively) upon micellization. However, no cross-peaks were observed for these pairs of protons in the 2D NOESY map shown in Figure 6. It suggests that the naphthyl rings are packed radiating outward with the part connected to alkyl chains closer than the part substituted by the sulfonate group, so that the distances among the negatively charged sulfonate groups are longer and the repulsion is weakened. That is why the changes in chemical shifts of H_a and H_c and the peak broadenings are smaller than those of H_b, H_d, and H_e. The same is the case of

the dramatical decrease in spin–spin relaxation times of H_b , H_d , and H_e , while those for the other aromatic protons are less affected by micellization.

Cross-peaks between H_b and H_g , between H_d and H_g , and between H_d and H_h appeared in Figure 3A. The interproton distances between H_d – H_g and H_d – H_h protons decreased from 4.65 and 6.95 to 3.5 and 3.7 Å, respectively (Table 3), upon micellization. These shortenings support the result obtained from relaxation measurements that H_g and a part of the H_h protons participate in the formation of the rigid surface layer of the hydrophobic micellar core.

Acknowledgment. Financial support by the Fundamental National Key Basic Research Development Program “Studies of the Extensively Enhanced Petroleum Recovery” (Project Grant G1999022504) is gratefully acknowledged.

References and Notes

- (1) Du, Y. R.; Zhao, S.; Shen, L. F. In *Annual Reports on NMR Spectroscopy*; Webb, G. A., Ed.; Academic Press: London, 2002; Vol. 48, Chapter 5, pp 145–194.
- (2) Cerichelli, G.; Mancini, G. *Curr. Opin. Colloid Interface Sci.*, **1997**, 2 (6), 641.
- (3) Macdonald, P. M. *Colloids Surf., A* **1999**, 147, 115.
- (4) Yuan, H. Z.; Cheng, G. Z.; Zhao, S.; Miao, X. J.; Yu, J. Y.; Shen, L. F.; Du, Y. R. *Langmuir* **2000**, 16, 3030.
- (5) Zhao, J.; Fung, B. M. *J. Phys. Chem.* **1993**, 97, 5185.
- (6) Sugiyama, K.; Esumi, K.; Koide, Y. *Langmuir* **1996**, 12, 6006.
- (7) Hawrylak, B. E.; Marangoni, D. G. *Can. J. Chem.* **1999**, 77, 1241.
- (8) Yuan, H. Z.; Zhao, S.; Cheng, G. Z.; Zhang, L.; Miao, X. J.; Mao, S. Z.; Yu, J. Y.; Shen, L. F.; Du, Y. R. *J. Phys. Chem. B* **2001**, 105, 4611.
- (9) Wang, T. Z.; Mao, S. Z.; Miao, X. J.; Zhao, S.; Yu, J. Y.; Du, Y. R. *J. Colloid Interface Sci.* **2001**, 241, 465.
- (10) Gao, H. C.; Zhao, S.; Mao, S. Z.; Yuan, H. Z.; Yu, J. Y.; Shen, L. F.; Du, Y. R. *J. Colloid Interface Sci.* **2002**, 249, 200.
- (11) Gjerd, M. I.; Nerdal, W.; Hoiland, H. *J. Colloid Interface Sci.* **1996**, 183, 285.
- (12) Yuan, H. Z.; Luo, L.; Zhang, L.; Zhao, S.; Mao, S. Z.; Yu, J. Y.; Shen, L. F.; Du, Y. R. *Colloid Polym. Sci.* **2002**, 280, 479.
- (13) Canet, D.; Mahieu, N.; Tekely, P. *J. Am. Chem. Soc.* **1992**, 114, 6190.
- (14) Belmajdoub, A.; Mahieu, N.; Tekely, P.; Canet, D. *J. Phys. Chem.* **1992**, 96, 1011.
- (15) Palmas, P.; Tekely, P.; Mutzenhardt, P.; Canet, D. *J. Chem. Phys.* **1993**, 99, 4775.
- (16) Mahieu, N.; Tekely, P.; Canet, D. *J. Phys. Chem.* **1993**, 97, 2764.
- (17) Raulet, R.; Furo, I.; Brondeau, J.; Diter, B.; Canet, D. *J. Magn. Reson.* **1998**, 133, 324.
- (18) Yuan, H. Z.; Miao, X. J.; Zhao, S.; Shen, L. F.; Yu, J. Y.; Du, Y. R. *Magn. Reson. Chem.* **2001**, 39, 33.
- (19) Ernst, R. R.; Bodenhausen, G.; Wokaun, A. *Principles of Nuclear Magnetic Resonance in One and Two Dimensions*; Oxford University Press: New York, 1987.
- (20) Zhao, S.; Yuan, H. Z.; Yu, J. Y.; Du, Y. R. *Colloid Polym. Sci.* **1998**, 276, 1125.
- (21) Bujake, J. E.; Goddard, E. D. *Trans. Faraday Soc.* **1965**, 61, 190.
- (22) Gerschman, J. W. *J. Phys. Chem.* **1957**, 61, 581.
- (23) Clifford, J. *Trans. Faraday Soc.* **1965**, 61, 1279.
- (24) Guo, W.; Li, Z.; Fung, B. M.; O'Rear, E. A.; Harwell, J. H. *J. Phys. Chem.* **1992**, 96, 6738.
- (25) Goon, P.; Das, S.; Clemett, C. J.; Tiddy, G. J. T.; Kumar, V. V. *Langmuir* **1997**, 13, 5577.
- (26) Berlot, I.; Chevalier, Y.; Labbe, P.; Moutet, J. C. *Langmuir* **2001**, 17, 2639.
- (27) Gao, Z.; Wasylshen, R. E.; Kwak, J. C. T. *J. Colloid Interface Sci.* **1990**, 137, 137.
- (28) Yuan, H. Z.; Du, Y. R.; Zhao, S.; Yu, J. Y. *Sci. China, Ser. A: Math., Phys., Astron.* **1999**, 42, 319.
- (29) Das, S.; Bhirad, R. G.; Nayyar, N.; Narayan, K. S.; Kumar, V. V. *J. Phys. Chem.* **1992**, 96, 7454.